
FOR THE RECORD

Solution structure of a novel calcium binding protein, MTH1880, from *Methanobacterium thermoautotrophicum*

CHANG-HUN LEE,^{1,3} JIN-WON JUNG,^{1,3} ADELINDA YEE,²
CHERYL H. ARROWSMITH,² AND WEONTAE LEE¹

¹Department of Biochemistry, College of Science, Yonsei University, Seoul, Korea, 120-749

²Ontario Cancer Institute and Department of Medical Biophysics, University of Toronto, Toronto, Ontario, Canada M5G 2M9

(RECEIVED October 3, 2003; FINAL REVISION December 20, 2003; ACCEPTED December 22, 2003)

Abstract

MTH1880 is a hypothetical protein from *Methanobacterium thermoautotrophicum*, a target organism of structural genomics. The solution structure determined by NMR spectroscopy demonstrates a typical $\alpha + \beta$ -fold found in many proteins with different functions. The molecular surface of the protein reveals a small, highly acidic pocket comprising loop B (Asp36, Asp37, Asp38), the end of β 2 (Glu39), and loop D (Ser57, Ser58, Ser61), indicating that the protein would have a possible cation binding site. The NMR resonances of several amino acids within the acidic binding pocket in MTH1880, shifted upon addition of calcium ion. This calcium binding motif and overall topology of MTH1880 differ from those of other calcium binding proteins. MTH1880 did not show a calcium-induced conformational change typical of calcium sensor proteins. Therefore, we propose that the MTH1880 protein contains a novel motif for calcium-specific binding, and may function as a calcium buffering protein.

Keywords: NMR spectroscopy; *Methanobacterium thermoautotrophicum*; calcium binding; structural proteomics

In the postgenomic era, it is now possible to use structural biology methods to annotate gene function before a new gene or protein is well characterized (Kim 1998). Attempts to do this on a large, even genome-wide scale have already started to yield structure-based, functional annotations for hypothetical proteins (Kennedy et al. 2002). Very recently, a number of structural genomics (or proteomics) efforts have provided correlations between biological function and fold classification for unknown gene products (Yang et al. 2003). In addition, the development of high-throughput

technologies, for protein purification and structure determination, enables the determination of new protein structures in a short period of time, often revealing previously unknown biochemical functions as well as cellular mechanisms of new gene products (Zhang and Kim 2003).

As part of an on-going structural genomics effort on proteins from the thermophilic methanogen, *Methanobacterium thermoautotrophicum* (Christendat et al. 2000), we have determined the solution structure of MTH1880. MTH1880 is a hypothetical protein from *M. thermoautotrophicum*, and shares high sequence similarity to only one other protein, Y858, from *Methanococcus janaschii* (~80% sequence identity). However, the molecular function and structure of Y858 are still unknown. The solution structure was searched for structural homologs, which may indicate clues to its biochemical or cellular function. From its molecular surface and charge distribution, we identified a putative cation, calcium binding site.

Reprint requests to: Weontae Lee, Department of Biochemistry, College of Science, Yonsei University, 134 Seodaemoon-Gu, Shinchon-dong, Seoul, Korea 120-749; e-mail: wlee@spin.yonsei.ac.kr; fax: 82-2-363-2706.

³These authors equally contributed to this work.

Article and publication are at <http://www.proteinscience.org/cgi/doi/10.1110/ps.03472104>.

Results

NMR resonance assignments and secondary structures

Resonance assignments of all backbone resonances were made using HNCA, HNCACB, CBCA(CO)NNH, and HN(CO)CA data. Most of the side-chain assignments were accomplished by combined use of 3D HCCH-TOCSY and ^{15}N -edited TOCSY-HSQC experiments. Secondary structures were readily identified from the chemical shift index (CSI; Wishart and Sykes 1994; Wishart et al. 1995) and NOE information (Wagner et al. 1986). The secondary structure of MTH1880 consisted of a three-stranded antiparallel β -sheet (residues 6–11, 39–44, and 51–55) and three short α -helices (residues 22–30, 63–73, and 82–87). A number of hydrogen bonds are found within the main-chain atoms of the secondary structures.

Solution structure of MTH1880

Most of the residues involved in forming the hydrophobic core of MTH1880 are found between the β -sheets ($\beta 3$ and $\beta 4$) and Helix 2. Although Helix 1 participates in the formation of the hydrophobic core, it has a dynamic feature based on rapid amide hydrogen exchange rates. Helix 3 at the C terminus packs against the β -sheets to cover the hydrophobic core residues (Fig. 1). There are five loops, comprising residues 12–21, 31–38, 45–50, 56–64, and 74–81. Interestingly, the charged residues in these loops endow MTH1880 with a strong dipolar nature. Two loops (B [31–38] and D [56–64]) generate a highly acidic surface on the protein, whereas loop C (45–50) and loop E (74–81) create a highly basic surface. The loops B–D are rather rigid rela-

tive to those of the loops C–E, which might provide some clues to infer the molecular function of MTH1880.

Structure–function of MTH1880

MTH1880 is classified as typical “ α and β ($\alpha + \beta$)” fold with antiparallel β -sheets (segregated α and β regions), common to many proteins with various functions (Murzin 1995). Structural homologs of MTH1880 were searched for using the DALI and SCOP servers. No structural homologs were identified for MTH1880 from the DALI search. However, several proteins were identified from a SCOP classification. Five structural folds, SH2-like, profilin, actin depolarizing, ferredoxin-like, and crystallin-like folds, were found based on the structural diversity (Fig. 2). To gain insight about the biochemical function of MTH1880, we investigated the molecular surface for potential ligand binding pockets. The Connolly surface of MTH1880 reveals a highly acidic pocket comprised of loop B (Asp36, Asp37, Asp38), the end of Helix 2 (Glu39), and loop D (Ser57, Ser58, Ser61). Because the total surface charge calculated with the Delphi module of InsightII is -3 , it could be possible that the negative charged cluster is a putative cation binding site. For further investigation, we performed ^{15}N - ^1H HSQC and HCCH-TOCSY experiments in the presence of divalent cations. For the case of Mg^{2+} ion, no spectral change was observed during titration. For Ca^{2+} ion, the resonance frequencies of a number of residues (Asp37 and Asp38 in loop B, Glu39 in Helix 2, and Leu56, Ser57, Ser58, Tyr59, and Asn60 in loop D) were changed (Fig. 3), indicative of Ca^{2+} binding to the acidic pocket of the protein.

Chemical shift perturbations of side-chain atoms during Ca^{2+} titration were more evident in HCCH-TOCSY spectra (data not shown). In the presence of Ca^{2+} , the side-chain resonances of Asp37, Glu39, Leu56, Ser57, and Tyr59 disappeared, whereas the line width of Ser58 was broadened upon Ca^{2+} addition. These residues are located on the acidic pocket comprising of loops B and D. Based on these observation, we indicate that MTH1880 binds Ca^{2+} specifically, and the Ca^{2+} binding site is located on the B–D loop region.

Because the resonances of the secondary structural elements were largely unchanged, indicating little or no change in the structured part of the protein, we could readily construct a calcium-bound model. The mode of calcium binding was inferred from the model of the calcium-bound structure (Fig. 4A). The carboxylic groups of Asp37 and Glu39 provide a coordination of the negative charges for the calcium cation (Fig. 4B). The carbonyl or hydroxyl groups of other residues are also involved in the interaction with calcium ion. The rigid conformations of loops B and D provide a well-defined binding site for calcium. This binding mechanism is also found in those of other calcium binding proteins, especially thermitase (Fig. 4C; Table 2). Ther-

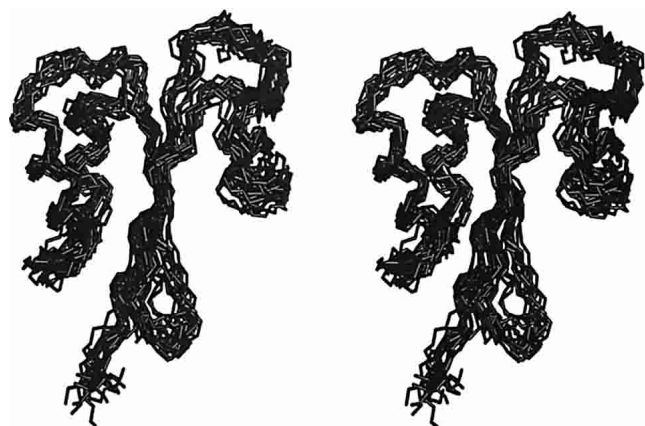


Figure 1. Solution structure of MTH1880. The backbone superposition of 20 final simulated annealing structures is displayed in stereo view.

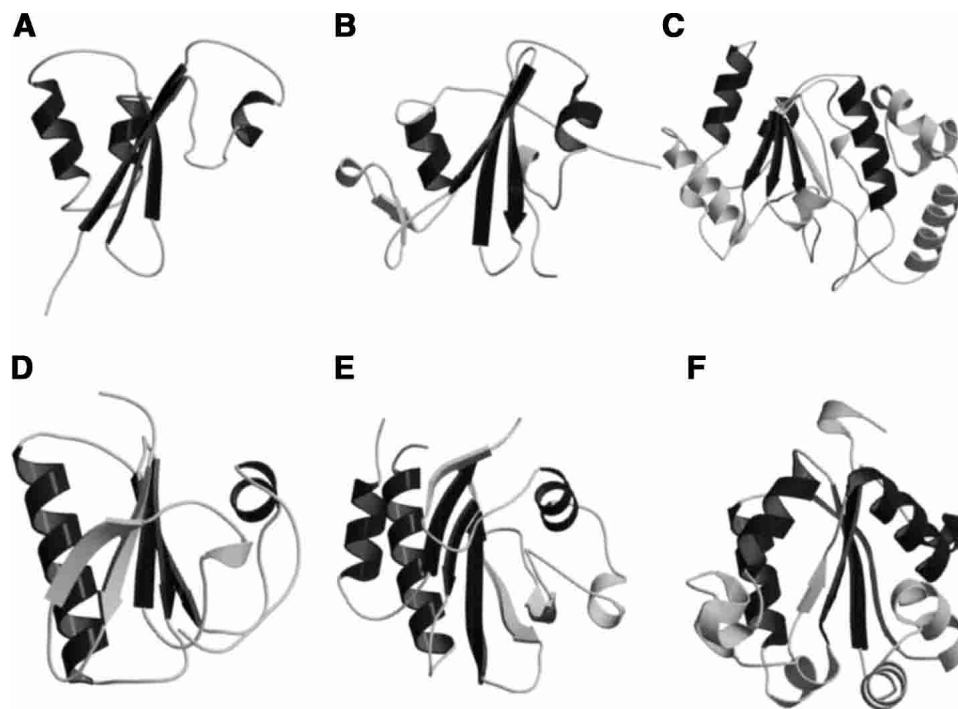


Figure 2. The proteins with the $\alpha + \beta$ fold displayed in ribbon diagram together with MTH1880. All structures were based on the results of SCOP classification. (A) MTH1880 showing secondary structural topology, (B) SH2 domain of C-ABL (PDB: 1AB2), (C) uracil-DNA glycosylase (PDB: 1UDI), (D) severin domain 2 (PDB: 1SVY), (E) profilin (PDB: 1PNE), (F) nucleoside diphosphate kinase (PDB: 1EHW). The overall structures of SH2 and gelsolin are very similar to that of MTH1880; however, two proteins have different function. The structures are generated by MOLMOL (Koradi et al. 1996), MOLSCRIPT (Kraulis 1991), and Raster3D (Merritt and Bacon 1997) programs.

mitase possesses a number of binding pockets for calcium ions formed by loop residues (Teplyakov et al. 1990). This model indicates that MTH1880 has a common feature with many well-characterized calcium binding proteins, but that MTH1880 itself contains a novel motif for calcium binding.

Discussion

MTH1880 has a common $\alpha + \beta$ type of fold similar to that found in many proteins with diverse functions. To define the biochemical function of MTH1880, we focused on a readily visible, small acidic binding pocket formed by loops B and D. Although MTH1880 has no classical cation binding motif, such as an EF-hand, a typical motif search indicates that the molecular shape and electric potential surface is typical of divalent cation binding capabilities. However, the calcium binding motif and overall topology of MTH1880 are different from those of other calcium binding proteins. Modeling of potential cations into the acidic pocket showed that the calcium ion fits well, but the magnesium ion does not, even though the magnesium ion is smaller than the calcium ion. These data may indicate that MTH1880 is a calcium specific protein. The cation specificity derived

from the “size-exclusion” effect is commonly observed in calcium binding proteins with the EF-hand motif (Snyder et al. 1990). To identify the potential biological role for MTH1880, we have searched calcium binding proteins with various functions. NMR studies for both synaptotagmin and syntaxin proteins showed that Ca^{2+} binding effect to these proteins occurs only via the side-chain atoms, not the backbone atoms (Shao et al. 1998). This property is very similar to that of MTH1880.

SCOP results showed that the orientation of secondary structural elements and the calcium-binding motif of gelsolin are very similar to those of MTH1880. However, the calcium ion induces a functionally important conformational change in gelsolin. It has been known that calcium-buffering proteins do not undergo a conformational change in the presence of the calcium ion (Rajini et al. 2001), indicating that MTH1880 could be a Ca^{2+} -buffering protein. Because MTH1880 has sequence homology with Y858 (~80%) from *M. janashii*, we propose that Y858 may also be a calcium-buffering protein and possess a similar molecular topology with MTH1880. Therefore, we propose the two hypothetical proteins, MTH1880 and Y858, could play a role in the control of archaeal calcium concentration through a calcium-buffering mechanism.

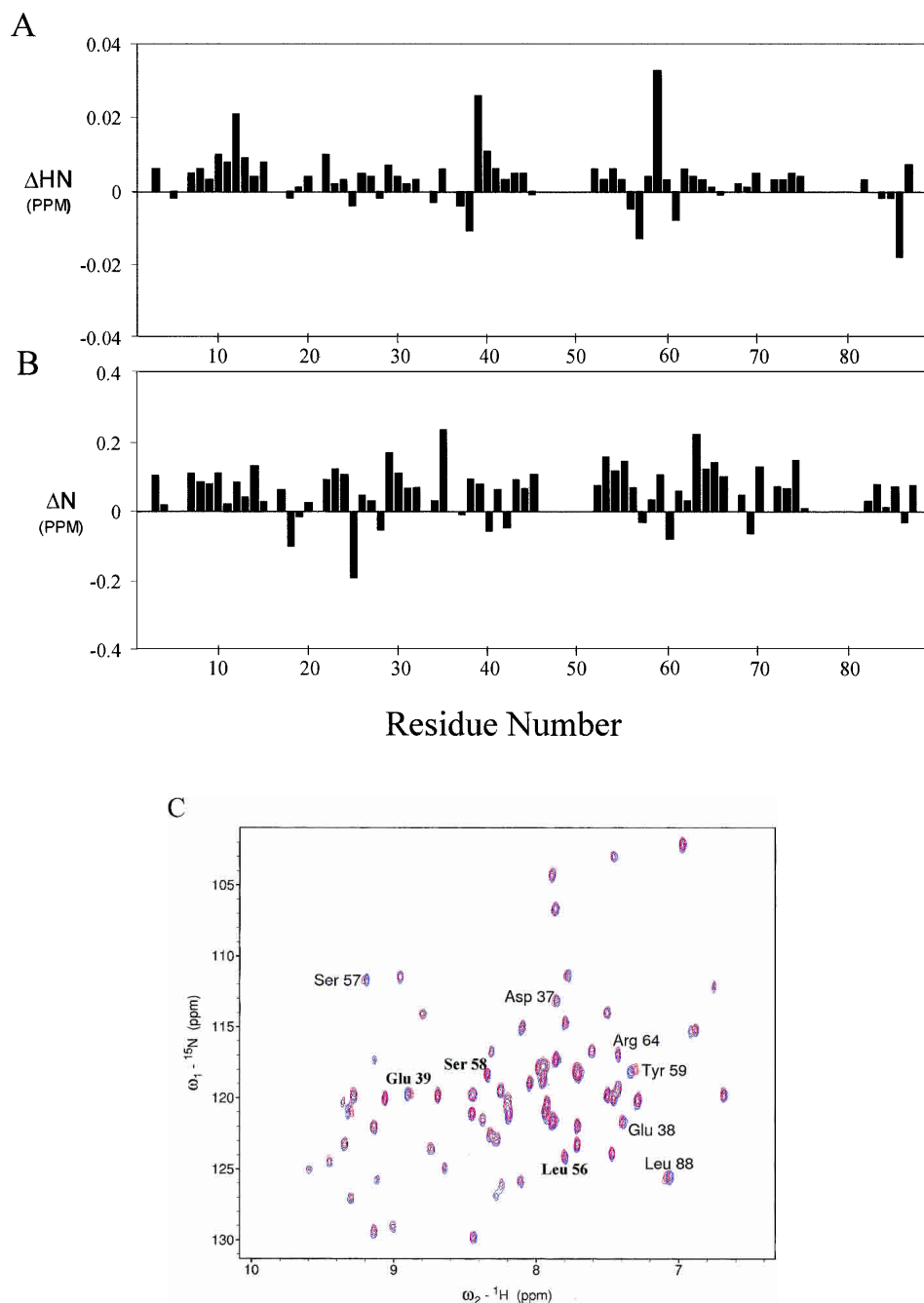


Figure 3. Chemical shift differences of (A) backbone amide proton and (B) nitrogen chemical shifts between free and calcium-bound form. The chemical shift difference (ppm) was calculated from the absolute value of the change in the ^1H chemical shift and ^{15}N chemical shift. (C) A superposition of the 2D ^1H - ^{15}N HSQC spectra in the presence (red) and absence (blue) of calcium ions.

Materials and methods

Gene cloning, protein expression, and purification

The MTH1880 gene was obtained from *M. thermoautotrophicum* ΔH genomic DNA by PCR amplification and subcloned into pET13b plasmid (Novagen Inc.) at the NdeI and BamHI sites. This

construct contains a hexahistidine tag (HisTag) with a thrombin cleavage site in the N-terminal extension.

The protein was overexpressed in the *Escherichia coli* strain BL21(DE3) pLysS and transformed with the pET13b/MTH1880 plasmid construct. Cells were grown on M9 minimal medium with $^{15}\text{NH}_4\text{Cl}$ and/or $[\text{U}-^{13}\text{C}]$ -glucose (Cambridge Isotope Laboratories Inc.) at 37°C . For optimum growth condition, thiamine 0.1% (W/V) and ampicillin, with a final concentration of 50 $\mu\text{g}/\text{mL}$, were

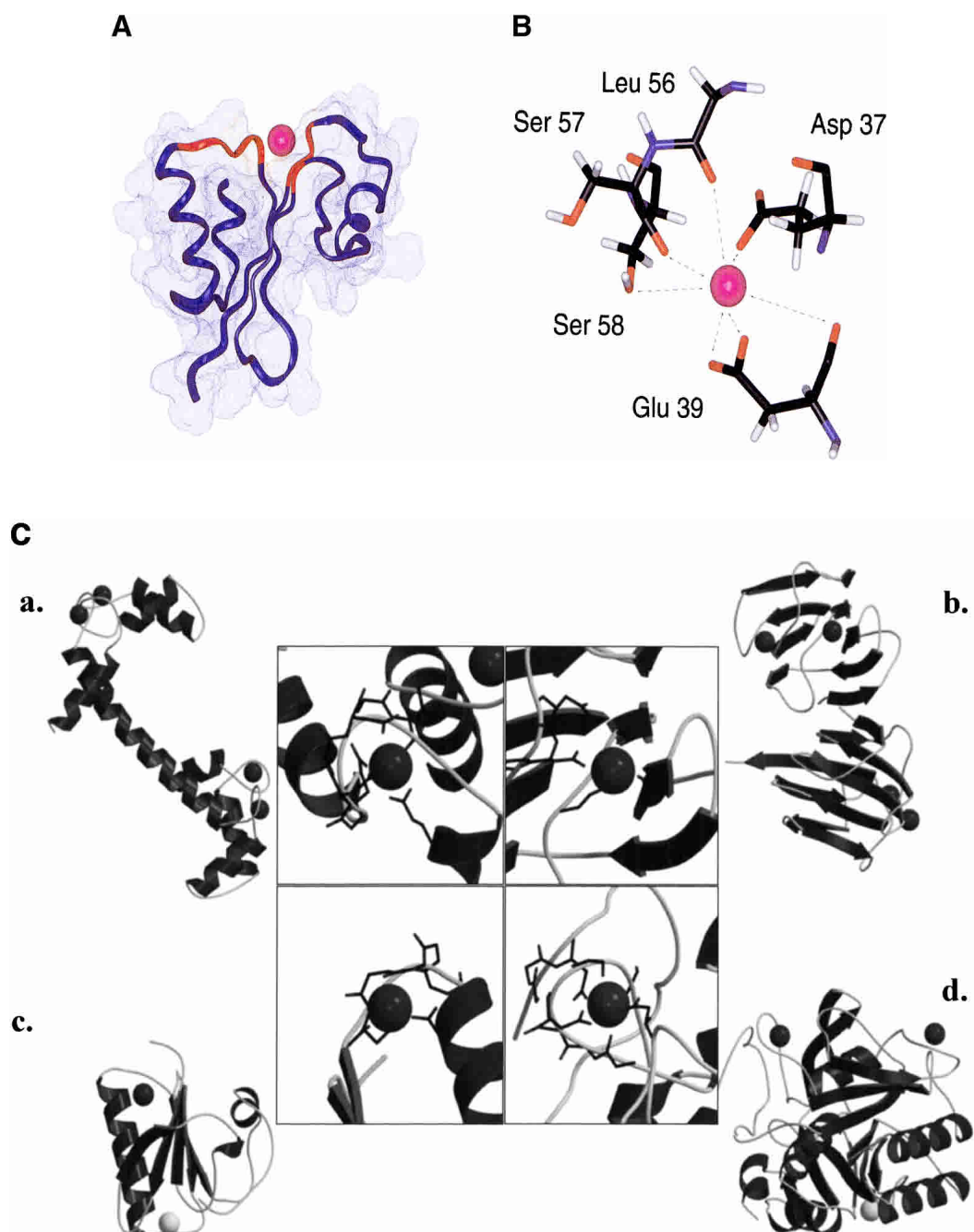


Figure 4. Calcium binding motif of MTH1880. (A) The structural model of MTH1880 bound to a calcium ion. Regions in red color represent the residues whose resonances changed upon calcium binding. (B) Proposed coordination of the calcium binding site based on NMR data. The residues involved in calcium binding were displayed with side-chain atoms. (C) A class of calcium binding motifs. (a) Calmodulin (PDB: 3CLN), (b) crystallin (PDB: 1HDF), (c) gelsolin (PDB: 4CPV), and (d) thermitase (PDB: 1THM). The calcium ion is shown as a black sphere and sodium ion as a white sphere.

added. Proteins were induced with 0.7 mM isopropyl β -D-thiogalactoside (IPTG) when A_{600} was reached at 0.6. Cells were harvested by centrifugation at $6700 \times g$ for 30 min, and resuspended in 25 mL of binding buffer (5 mM imidazole, 10 mM Tris, 500 mM NaCl, 1 mM PMSF, in pH 8.0) and sonicated. The lysate was centrifuged at $17,500 \times g$ for 30 min and the insoluble material was removed. The supernatant was applied to a His-Bind Resin (No-

vagen Inc.); bound protein was washed with 12 volumes of 30 mM imidazole and eluted with 300 mM imidazole. To remove His-Tag, the protein solution was incubated with bovine thrombin (Pharmacia Biotech Inc.) in the ratio of 10 Unit/mg at 25°C for 6 h. After thrombin digestion, gel filtration was performed using HiLoad 16/60 Sephadex 75 column (Pharmacia Biotech Inc.). In this procedure, the loading buffer was used with the NMR buffer (25

Table 1. Structural restraints and statistics for the NMR structures

Restraints for structure calculation		
Total NOE restraints		723
Intraresidue		275
Sequential		162
Medium range ($1 < i - j \leq 5$)		89
Long range ($ i - j > 5$)		143
Hydrogen bonds		54
Dihedral angles (ϕ)		39
Statistics for structure calculations		
RMSD from distance restraints		
NOE restraints (Å)		0.016 ± 0.006
Dihedral restraints ($^\circ$)		0.46 ± 0.42
RMSD from idealized geometry		
Bonds (Å)		0.016 ± 0.003
Angle ($^\circ$)		0.35 ± 0.03
Impropers ($^\circ$)		0.19 ± 0.06
Mean energies (kcal/mole)		
E_{total}		75.27 ± 19.50
E_{bond}		3.89 ± 1.33
E_{angle}		50.67 ± 8.78
E_{vdw}		7.81 ± 7.61
E_{noc}		11.40 ± 7.26
E_{dih}		0.91 ± 0.91
RMSD of atomic coordinates (Å)		
	Backbone	Heavy atoms
$\langle \text{SA} \rangle_k^a$ vs. $\langle \text{SA} \rangle_{kr}$		
All residues	1.195	1.907
Secondary structures	0.747	1.292

^a $\langle \text{SA} \rangle_k$ is the ensemble of 20 final simulated annealing structures of MTH1880.

$\langle \text{SA} \rangle_{kr}$ is the mean structure obtained by averaging the individual structures following a superimposition of the backbone heavy atoms.

mM sodium phosphate, 300 mM NaCl, 0.002% NaN₃). The purified protein was concentrated to approximately 2 mM with Centricon-3 concentrators (Millipore Inc.).

NMR spectroscopy

NMR spectra were recorded at 500 MHz Varian UNITY Inova or on Bruker DRX500 with a triple resonance probe. All experiments were conducted at 37°C. 2D ¹⁵N-¹H HSQC (Kay et al. 1992) and 3D ¹⁵N-edited NOESY-HSQC and TOCSY-HSQC experiments were performed on [U-¹⁵N]-labeled MTH1880. 3D HNCA, 3D

HNCACB, HN(CO)CA, CBCA(CO)NH (Muhandiram and Kay 1994), HCCH-TOCSY (Kay et al. 1993), and ¹³C-edited NOESY-HSQC experiments were conducted on [U-¹³C, U-¹⁵N]-labeled MTH1880. A lyophilized sample of [U-¹⁵N] MTH1880 was reconstituted in D₂O solution to monitor the exchange of backbone amide protons using the ¹⁵N-¹H HSQC experiment. Backbone vicinal coupling constants were measured using the 3D HNHA experiment (Kuboniwa et al. 1994). All data were processed with NMRPipe (Delaglio et al. 1995) and analyzed with the Sparky program (Goddard and Kneller 2003).

Structure calculations

Structure calculations were carried out using the hybrid distance geometry and dynamical simulated annealing protocol (Nilges et al. 1998) using the program CNS 1.0 (Brunger et al. 1998) on a Linux workstation. Cross-peaks in NOESY spectra were classified as strong, medium, and weak intensities, corresponding to upper bounds of 2.5, 3.0, 4.0, or 5.0 Å for distance constraints. In addition, the pseudo-atom corrections for methylene, methyl groups, and aromatic ring protons were made during structure calculations (Wüthrich et al. 1983). For ³J_{HNα} > 8 Hz, ϕ was restrained to $-120(\pm 40)^\circ$ and for ³J_{HNα} < 6 Hz, ϕ was restrained to $-57(\pm 20)^\circ$. Hydrogen bond constraints for slow exchanging amide protons ($d_{\text{O-HN}} = 1.8\text{--}2.2$ Å, $d_{\text{O-N}} = 2.8\text{--}3.3$ Å) were also used during structural calculations.

Initially, a set of 50 structures were generated by a simulated annealing protocol in the CNS program, and the 20 structures with the lowest energy were selected for further analysis. Structural search of MTH1880 were performed manually with SCOP (Murzin et al. 1995) and automatically with Dali (Holm and Sander 1995).

Molecular modeling for calcium binding

The average structure $\langle \text{SA} \rangle_k$ was calculated from the geometric average of 20 $\langle \text{SA} \rangle_k$ structure coordinates and subjected to a restrained energy minimization (REM) structure, yielding an $\langle \text{SA} \rangle_{kr}$ structure of MTH1880. The starting structure for the Ca²⁺ bound form was constructed with $\langle \text{SA} \rangle_{kr}$. Using the cvff force field, a structure with the calcium ion was modeled and further optimized by the molecular dynamics simulation, using the InsightII program and DISCOVER 3 module (Accelrys Inc.). Initially, the calcium ion was located adjacent to the negatively charged region of the protein, but no specific distance restraints were imposed between the calcium ion and protein; except the electrostatic interaction between the calcium ion and side-chain atoms of the protein. To obtain the lowest energy conformation with calcium ion, a re-

Table 2. Biochemical and structural data of calcium binding proteins

	Characteristic motif	Structural feature	Involved amino acids	Conformational change after Ca ²⁺ -binding	Function (with Ca ²⁺)
MTH1880	—	Beta-sheets and loops	D, E, S, L	N	Calcium buffer
Gelsolin	—	Beta-sheet, loop and helix	D, G, P	Y	Actin-binding
Calmodulin	EF-hand	Helix-loop-helix	D, E, Q, N, T	Y	Calcium sensor
Thermitase	Subtilisin family	Loops	D, Q, R, S, T, A, Y, V, I	Y	Thermostability
Crystallin	Greek key	Beta-sheets	D, E, N, Q, K, S, Y	N	Calcium buffer

Source: structural features and characters are reported as followed: Gelsolin (PDB: 1SVY, 1D0N), Calmodulin (PDB: 3CLN), Thermitase (PDB: 1THM, reference cited in text: 17), γ -Crystallin (PDB: 1HDF).

strained molecular dynamics simulation was performed for 250 psec at 298 K. During the dynamics simulation, the structural ensemble was sampled every 100 intervals (0.1 psec). Finally, the lowest energy conformation was optimized by restraint energy minimization, with the BFG method, until the deviation of its energy gradient reached $0.001 \text{ kcal mole}^{-1}$.

Accession numbers

Backbone and side-chain chemical shift assignments for MTH1880 have been deposited to BioMagResBank (accession code BMRB-5129). Coordinates for the 20 structures and ensemble structure have been deposited in the RCSB PDB with accession code 1IQO and 1IQS, respectively.

Acknowledgments

This study was supported by the Ministry of Science and Technology of Korea/the Korea Science and Engineering Foundation through the NRL program of MOST NRDP (M1-0203-00-0020); the Ministry of Education and Human Resource through the BK21 project (W.L.); the Ontario Research and Development Challenge Fund; and Genome Canada (C.H.A.).

The publication costs of this article were defrayed in part by payment of page charges. This article must therefore be hereby marked "advertisement" in accordance with 18 USC section 1734 solely to indicate this fact.

References

- Brunger, A.T., Adams, P.D., Clore, G.M., DeLano, W.L., Gros, P., Grosse-Kunstleve, R.W., Jiang, J.S., Kuszewski, J., Nilges, M., Pannu, N.S., et al. 1998. Crystallography and NMR system: A new software suite for macromolecular structure determination. *Acta Crystallogr. D. Biol. Crystallogr.* **54**: 905–921.
- Christendat, D., Yee, A., Dharamsi, A., Kluger, Y., Savchenko, A., Cort, J.R., Booth, V., Mackereth, C.D., Saridakis, V., Ekiel, I., et al. 2000. Structural proteomics of an archaeon. *Nat. Struct. Biol.* **7**: 903–909.
- Delaglio, F., Grzesiek, S., Vuister, G.W., Zhu, G., Pfeifer, J., and Bax, A. 1995. NMRPipe: A multidimensional spectral processing system based on UNIX pipes. *J. Biomol. NMR* **6**: 277–293.
- Goddard, T.D. and Kneller, D.G. 2003. SPARKY 3. University of California, San Francisco, CA.
- Holm, L. and Sander, C. 1995. Dali: A network tool for protein structure comparison. *Trends Biochem. Sci.* **20**: 478–480.
- Kay, L.E., Keifer, P., and Saarinen, T. 1992. Pure absorption gradient enhanced heteronuclear single quantum correlation spectroscopy with improved sensitivity. *J. Am. Chem. Soc.* **114**: 10663–10665.
- Kay, L.E., Xu, G., Singer, A.U., Muhandiram, D.R., and Forman-Kay, J.D. 1993. A gradient-enhanced HCCH-TOCSY experiment for recording side-chain ^1H and ^{13}C correlations in H_2O samples of proteins. *J. Magn. Reson. Ser. B* **101**: 333–337.
- Kennedy, M.A., Montelione, G.T., Arrowsmith, C.H., and Markley, J.L. 2002. Role for NMR in structural genomics. *J. Struct. Funct. Genomics* **2**: 155–169.
- Kim, S.H. 1998. Shining a light on structural genomics. *Nat. Struct. Biol.* **5**: 643–645.
- Koradi, R., Billeter, M., and Wüthrich, K. 1996. MOLMOL: A program for display and analysis of macromolecular structures. *J. Mol. Graph.* **14**: 29–32.
- Kraulis, P.J. 1991. MOLSCRIPT: A program to produce both detailed and schematic plots of protein structures. *J. Appl. Crystallogr.* **24**: 946–950.
- Kuboniwa, H., Grzesiek, S., Delaglio, F., and Bax, A. 1994. Measurement of HN-H α J couplings in calcium-free calmodulin using new 2D and 3D water-flip-back methods. *J. Biomol. NMR* **4**: 871–878.
- Merritt, E.A. and Bacon, D.J. 1997. Raster3D: Photorealistic molecular graphics. *Methods Enzymol.* **277**: 505–524.
- Muhandiram, D.R. and Kay, L.E. 1994. Gradient-enhanced triple-resonance three-dimensional NMR experiments with improved sensitivity. *J. Magn. Reson. Ser. B* **103**: 203–216.
- Murzin, A.G., Brenner, S.E., Hubbard, T., and Chothia, C. 1995. SCOP: A structural classification of proteins database for the investigation of sequences and structures. *J. Mol. Biol.* **247**: 536–540.
- Nilges, M., Clore, G.M., and Gronenborn, A.M. 1988. Determination of three-dimensional structures of proteins from interproton distance data by hybrid distance geometry-dynamical simulated annealing calculations. *FEBS Lett.* **229**: 317–324.
- Rajini, B., Shridas, P., Sundari, C.S., Muralidhar, D., Chandani, S., Thomas, F., and Sharma, Y. 2001. Calcium binding properties of γ -crystallin: Calcium ion binds at the Greek key β γ -crystallin fold. *J. Biol. Chem.* **276**: 38464–38471.
- Shao, X., Fernandez, I., Sudhof, T.C., and Rizo, J. 1998. Solution structures of the Ca^{2+} -free and Ca^{2+} -bound C2A domain of synaptotagmin I: Does Ca^{2+} induce a conformational change? *Biochemistry* **37**: 16106–16115.
- Snyder, E.E., Buoscio, B.W., and Falke, J.J. 1990. Calcium(II) site specificity: Effect of size and charge on metal ion binding to an EF-hand-like site. *Biochemistry* **29**: 3937–3943.
- Tepljakov, A.V., Kuranova, I.P., Harutyunyan, E.H., Vainshtein, B.K., Frommel, C., Hohne, W.E., and Wilson, K.S. 1990. Crystal structure of thermolysin at 1.4 Å resolution. *J. Mol. Biol.* **214**: 261–279.
- Wagner, G., Neuhaus, D., Worgotter, E., Vasak, M., Kagi, J.H., and Wüthrich, K. 1986. Nuclear magnetic resonance identification of "half-turn" and 3(10)-helix secondary structure in rabbit liver metallothionein-2. *J. Mol. Biol.* **187**: 131–135.
- Wishart, D.S. and Sykes, B.D. 1994. Chemical shifts as a tool for structure determination. *Methods Enzymol.* **239**: 363–392.
- Wishart, D.S., Bigam, C.G., Holm, A., Hodges, R.S., and Sykes, B.D. 1995. ^1H , ^{13}C and ^{15}N random coil NMR chemical shifts of the common amino acids. I. Investigations of nearest-neighbor effects. *J. Biomol. NMR* **5**: 67–81.
- Wüthrich, K., Billeter, M., and Braun, W. 1983. Pseudo-structures for the 20 common amino acids for use in studies of protein conformations by measurements of intramolecular proton–proton distance constraints with nuclear magnetic resonance. *J. Mol. Biol.* **169**: 949–961.
- Yang, Z., Savchenko, A., Yakunin, A., Zhang, R., Edwards, A., Arrowsmith, C., and Tong, L. 2003. Aspartate dehydrogenase, a novel enzyme identified from structural and functional studies of TM1643. *J. Biol. Chem.* **278**: 8804–8808.
- Zhang, C. and Kim, S.H. 2003. Overview of structural genomics: From structure to function. *Curr. Opin. Chem. Biol.* **7**: 28–32.